THESIS FOR THE DEGREE OF LICENTIATE OF ENGINEERING

Reference Signal Construction for Passive Synthetic Aperture Radar from Digital Video Broadcasting Signals with Samples Missing

ANDERS HAGLUND

Department of Space, Earth and Environment
CHALMERS UNIVERSITY OF TECHNOLOGY
Gothenburg, Sweden 2026

Reference Signal Construction for Passive Synthetic Aperture Radar from Digital Video Broadcasting Signals with Samples Missing
ANDERS HAGLUND

Department of Space, Earth and Environment
Chalmers University of Technology
SE-412 96 Gothenburg
Sweden
Telephone: +46 (0)31-772 1000

Chalmers digitaltryck
Gothenburg, Sweden 2026

Reference Signal Construction for Passive Synthetic Aperture Radar from Digital Video Broadcasting Signals with Samples Missing

ANDERS HAGLUND
Department of Space, Earth and Environment
Chalmers University of Technology

Abstract

In this thesis, an improved reference signal for making passive Synthetic Aperture Radar (SAR) images is constructed by demodulating a Digital Video Broadcasting-Terrestrial (DVB-T digital TV) signal received on a flying platform with a portion of the samples missing. The quality of the reference signal affects the quality of the passive SAR image, so the reference signal needs to be of good quality. Demodulating the DVB-T signal received in the flying platform for constructing the reference signal makes the passive SAR system less complex than using a receiver on an additional, stationary platform for that purpose. A novel algorithm for demodulating a DVB-T signal with samples missing is presented and is shown to work for constructing a good reference signal. Signals received by the airborne SAR system LORA, developed by the Swedish Defence Research Agency (FOI), are used. LORA cannot register received samples completely continuously but about 1 % of the samples are missing. The demodulated signal is then manipulated and modulated again to make a reference signal that is shown to suppress artefacts from the signal structure in an example SAR image.

Synthetic aperture radar is a useful technology for making radar images. Passive SAR does not transmit signals but instead use signals from other, possibly non-cooperative transmitters. Passive SAR has some desirable characteristics compared to conventional active SAR, for example, the cost and weight of the radar system may be lower as it does not have a transmitter. A passive SAR may also use frequencies that are not available for radar purposes and that may interact differently with the environment, e.g. frequencies sufficiently low to penetrate foliage. The passive SAR image is produced using measurements of received echo returns while the transmitter or the receiver is moving. In addition to the measured of echoes, the corresponding (measured) positions of the antennas are needed together with a measured reference signal from the transmitting source. The SAR image is formed by correlating the received echo returns with the reference signal which ideally should be the same as the transmitted signal (or an intentionally modified copy of it). There are several different kinds of possible transmitters and signals available for passive SAR. In this thesis, signals that comply with the digital TV standard Digital Video Broadcasting-Terrestrial (DVB-T) are used. DVB-T signals are attractive for use in passive radar since, for example, the transmitted power is high (tens of kilowatts), signals are available in wide areas, in several countries and on several continents, their bandwidth and frequencies and their use of Orthogonal Frequency Division Multiplexing (OFDM) modulation which can be demodulated, decoded and corrected.

Keywords: passive radar, reference signal, passive Synthetic Aperture Radar (SAR), Digital Video Broadcasting-Terrestrial (DVB-T), Orthogonal Frequency Division Multiplexing (OFDM), signal reconstruction, missing samples

Acknowledgements

I am very grateful to my main supervisor Prof. Lars Ulander at the Department of Space, Earth and Environment and colleague at Totalförsvarets forskningsinstitut (Swedish Defence Research Agency, FOI) for offering me this opportunity of studying for a licentiate degree, for suggesting the topic, for providing resources, for inspiration and for believing in me.

I am also grateful to my assistant supervisor Dr. Per-Olov Frölind at FOI for interesting discussions, for helping me with the Synthetic Aperture Radar (SAR) images in section 5.5 and for reviewing and giving comments.

I would like to thank Dr. Peter Stenumgaard at FOI, who reviewed the first drafts of Paper B (as part of a course in writing for publication), for giving comments and for encouragement.

I would also like to thank my other colleagues working in the airborne synthetic aperture radar project at FOI: Anders Gustavsson for encouragement, Thomas Sjögren for company during the conference where paper A was presented and Rolf Ragnarsson for the co-operation during the flight campaigns.

Many thanks to Gunnar Stenström, previously at FOI, for help with managing the LORA system and the recorded data from it and Per Grahn at FOI for help with the equipment for handling the recorded data from LORA.

Many thanks also to Head of the Radar Systems Department Fredrik Lantz at FOI for encouragement and Head of Division Christian Jönsson at FOI for approving starting these licentiate studies.

I would also like to thank the people at Division of Geoscience and Remote Sensing at the Department of Space, Earth and Environment at Chalmers University of Technology who have helped me.

Finally, I would like to thank the pilots, technicians and other staff at Försvarets Materielverk (Swedish Defence Materiel Administration, FMV) for good co-operation during the flight campaigns with the airborne LORA system.

Appended Publications

This thesis is based on the following appended papers:

Paper A **A. Haglund**, P.-O. Frölind, and L. M. H. Ulander, "Simulation of effect of periodically missing samples on decoding in passive Synthetic Aperture Radar system using OFDM," in *Proc. IGARSS 2019 - 2019 IEEE International Geoscience and Remote Sensing Symposium*, Yokohama, Japan, 2019, pp. 2949-2952.

Paper B **A. Haglund**, P.-O. Frölind, and L. M. H. Ulander, "Recovery of missing samples in Orthogonal Frequency Division Multiplexing signals with optimisation using data carriers," *IET Radar, Sonar & Navigation*, vol. 18, no. 8, 2024, pp. 1217–1234.

Related Publications

The author has contributed to the following publications that are related to the work in this thesis but are not appended:

I P.-O. Frölind, A. Gustavsson, **A. Haglund**, R. Ragnarsson, and L. M. H. Ulander, "Analysis of a ground target deployment in an airborne passive SAR experiment," in *Proc. 2017 IEEE Radar Conference (RadarConf)*, Seattle, WA, USA, 2017, pp. 0273-0278, doi: 10.1109/RADAR.2017.7944211.

II L. M. H. Ulander, P.-O. Frölind, A. Gustavsson, **A. Haglund**, and R. Ragnarsson, "Passive synthetic-aperture radar for detection of ground vehicles," in *Proc. International Conference on Radar Systems (Radar 2017)*, Belfast, UK, 2017, pp. 1-4, doi: 10.1049/cp.2017.0458.

III T. K. Sjögren, P.-O. Frölind, R. Ragnarsson, **A. Haglund**, A. Gustavsson, L. M. H. Ulander, V. T. Vu, and M. I. Pettersson, "Simultaneous passive SAR imaging and detection of airborne targets," in *Proc. International Conference on Radar Systems (Radar 2017)*, Belfast, UK, 2017, pp. 1-5, doi: 10.1049/cp.2017.0502.

IV L. M. H. Ulander, P.-O. Frölind, A. Gustavsson, **A. Haglund**, and R. Ragnarsson, "Active and passive UHF-band SAR for ground surveillance," in *Proc. The European Conference on Synthetic Aperture Radar, EUSAR 2018*, Aachen, Germany, 2018, pp. 1481-1484.

V L. M. H. Ulander, A. R. Monteith, P.-O. Frölind, A. Gustavsson, **A. Haglund**, R. Ragnarsson, and G. Stenström, "Airborne SAR for calibration of P-band tower radar," in *Proc. IGARSS 2019 - 2019 IEEE International Geoscience and Remote Sensing Symposium*, Yokohama, Japan, 2019, pp. 541-544, doi: 10.1109/IGARSS.2019.8899069.

VI L. M. H. Ulander, P.-O. Frölind, A. Gustavsson, **A. Haglund**, R. Ragnarsson, and T. Sjögren, "Ground mapping using active and passive UHF-band SAR," in *Proc. 2020 IEEE International Radar Conference (RADAR)*, Washington, DC, USA, 2020, pp. 524-529, doi: 10.1109/RADAR42522.2020.9114844.

VII P.-O. Frölind, A. Gustavsson, **A. Haglund**, R. Ragnarsson, T. Sjögren, G. Stenström, and L. M. H. Ulander, "First results from airborne passive radar measurements and aircraft detection exploiting digital TV broadcast signals," in *Proc. 2024 International Radar Conference (RADAR)*, Rennes, France, 2024, pp. 1-5, doi: 10.1109/RADAR58436.2024.10993567.

VIII L. M. H. Ulander, P.-O. Frölind, A. Gustavsson, **A. Haglund**, O. Jonsson, R. Ragnarsson, and T. Sjögren, "Techniques for improving image quality of airborne passive synthetic aperture radar," in *Proc. 2025 IEEE Radar Conference (RadarConf25)*, Krakow, Poland, 2025, pp. 841-846, doi: 10.1109/RadarConf2559087.2025.11205084.

Contents

1 Introduction

A radar is a device that transmits electromagnetic signals and receives the echoes from objects [1]. Radar was from the beginning an acronym for RAdio Detection And Ranging.

Radars are present everywhere in society, in many different types, with many different abilities using a wide range of frequencies. There are many applications of radars. Radars are widely used for remote sensing, for surveillance and detection of changes over time. Examples of radar applications are radars used for missile defence, air traffic control, police traffic surveillance and weather radars for making weather forecasts [2].

The electromagnetic signals interact differently with the environment (through e.g. diffraction, reflection and attenuation [1]) depending on their frequency and polarisation, and radars are designed for selected frequencies and polarisations depending on their specific use, e.g. in all weather conditions or for foliage, ground or materials penetration. Radars can also measure the phase history of the radar echoes and their radial velocity (Doppler shift) [2]. This is used e.g. for detection of aircraft and missiles and for searching and tracking airborne targets. Radars are mounted on many different kinds of platforms, for example on spaceborne, airborne, naval and automotive platforms. With a synthetic aperture radar, maps over the reflectivity of the terrain and stationary targets in the terrain can be made and moving targets can be detected. With inverse synthetic aperture radar, images over the reflectivity of different parts of a target, seen from different angles, can be made. The radar antenna beamwidth is designed to be narrow (e.g. for tracking, mapping and for good angular resolution) or wide (e.g. for searching and for strip-map synthetic aperture radar) [1]. Radars are also designed to transmit the electromagnetic signals continuously or in pulses or not transmit at all (passive radars). Passive radars are used for e.g. air surveillance and have some advantages over conventional transmitting radars but it still remains to find applications of passive radars where they provide a clear advantage over conventional transmitting radars [3].

A passive radar is a radar that does not transmit itself but it uses echoes from radiation transmitted from other (non-cooperative or to some extent co-operative) transmitter(s), for example transmitters for Digital TV using the Digital Video Broadcasting-Terrestrial standard (section 1.3 below).

A Synthetic Aperture Radar (SAR) is used for making two- or three-dimensional images (section 1.2). Passive SAR is an emerging technology that can be used for mapping, surveillance and detection [4].

For extracting information from the received echoes, a radar most often compares (correlates) the received echoes with a reference signal which closely resembles the transmitted signal (section 2.3).

The types of radars considered in this thesis are passive radar and passive synthetic aperture radar (sections 1.1 and 1.2 below).

1.1 Passive radar

A transmitter used for passive radar may transmit broadcast or communication signals or it may be another radar transmitting radar signals. If the receiver and transmitter are

separated such a long distance that the radar has significantly different properties from a system with co-located receiver and transmitter, then it is also called a passive bistatic radar. There are also bistatic radar systems with their own transmitters using bistatic geometries. Early measurements with a passive bistatic arrangement using a broadcast signal were reported already in year 1924 [3].

Passive bistatic radars have a number of desirable characteristics compared to radars that transmit. The cost for a passive bistatic radar may be lower as the system does not have its own transmitter and since it does not transmit any energy. Also the weight is lower, which may be important for airborne systems. Since it does not transmit, it is more difficult to detect and no permission for transmitting signals is needed so it may use parts of the electromagnetic spectrum that are reserved for other uses than for radars. Moreover, the radar cross section in bistatic geometry is different and could provide an advantage, due to the separation of transmitter and receiver, against targets that are designed for having low mono-static radar cross section.

Passive bistatic radars also have some disadvantages compared to conventional active radars as the transmitted signal might not be intended for use in radars, for example the signal modulation, the frequency band used by the signal, coverage of illumination and emitted power are not optimised for radar use. Several different kinds of transmitting systems, signals and standards have been subject of research for use in passive radar applications, for example FM broadcast radio signals, analogue TV, digital TV and radio, mobile telephony systems, Wi-Fi and space-borne systems like global navigation satellite systems and satellite TV [3].

1.2 Synthetic aperture radar

A Synthetic Aperture Radar (SAR) is a radar that can produce an image by moving the receiver or transmitter antenna relative to the area to be imaged while recording radar echoes from several different positions along the path. An image is calculated from the recorded radar returns from the different receiver (or transmitter) positions, thus making up a synthesised aperture. The passive SAR image is produced using measurements of received echo returns and their corresponding (measured) positions together with a measured reference signal from a transmitting source and the positions of the source.

A passive SAR does not transmit itself but uses signals from illuminators of opportunity that possibly do not co-operate. Passive SAR has some desirable characteristics compared to conventional active SAR since no electromagnetic energy is transmitted, for example the cost and the weight for the radar system may be lower as it does not have a transmitter and it may use frequencies that are not available for radar purposes that may interact differently with the environment, e.g. frequencies sufficiently low to penetrate foliage. Moreover, passive SAR facilitates covert operation, not revealing that the area is under surveillance. The transmitter or the receiver is moving and the passive SAR uses bistatic geometry. Possible configurations to mention include [5] fixed transmitter on the ground and the receiver on an aircraft, transmitter on a satellite or aircraft and the receiver on the ground and transmitter on a satellite and the receiver on an aircraft. When using an airborne system, most often the system is flown along a linear or in some cases circular

path [5]. In systems with a moving receiver, the echo signals from the target area could be collected with a fixed antenna pointing broadside to the platform path (stripmap mode) or with an antenna steered towards a fixed location or target area (spotlight mode).

The airborne SAR research system LORA (chapter 5, developed by the Swedish Defence Research Agency (FOI)) has been used for both active and passive stripmap SAR. LORA cannot register received signals completely continuously but about 1 % of the samples are missing which is a problem that is discussed in this thesis. LORA was originally designed for active SAR using transmitted pulses, so there was no need for registering received signals continuously. Samples are stored in data packets together with descriptive information about each pulse. Samples are thrown away during the time the descriptive information is stored.

1.3 Digital TV in passive radar

A large amount of research has been carried out on passive radar using signals for digital TV. One digital TV standard that has been exploited is Digital Video Broadcasting-Terrestrial (DVB-T) from European Telecommunications Standards Institute [6]. Digital TV signals have several properties that are attractive for use in passive radar. The bandwidth of one signal is about 7.6 MHz (for 8 MHz channels [6]), giving a best resolution for passive SAR of about 20 m in range. The transmitted power is high (tens of kilowatts) and the frequency is in the UHF-band, typically between 470 and 860 MHz [7]. The DVB-T standard is in use worldwide, in several countries on several continents. It uses Orthogonal Frequency Division Multiplexing (OFDM) modulation with error correcting coding and resembles band-limited noise [7]. The transmitted signal can be reconstructed, for use as reference signal, by demodulating (extracting the subcarrier symbols) and decoding the received signal (using the in-built error correcting coding), then coding and modulating the signal again.

1.4 This thesis

In this thesis, a reference signal for passive SAR based on DVB-T signals is constructed for making passive SAR images. The DVB-T signal is reconstructed close to as it was when it was transmitted by demodulating the signal received in the LORA system's wide-beam antennas mounted on a flying aeroplane. The signal recorded by LORA misses a portion of the samples and these samples are reconstructed with a novel algorithm for reconstructing missing samples that is also presented. The reference signal is constructed by correcting the demodulated signal and then modulating it again with and without manipulating the signal for decreasing artefacts from the signal structure. Examples of passive SAR images calculated with the constructed reference signal with and without manipulation for decreasing artefacts are shown. The objective of this work is to improve the quality of passive SAR images by improving the reference signal constructed from signals received in the aeroplane.

2 Passive Radar basics

A bistatic radar is a radar where the transmitter and the receiver are separated a significant distance. This chapter provides basics of passive radar, specifically Passive Bistatic Radar (PBR). A frequently used alternative term is Passive Coherent Location (PCL). An introduction to passive bistatic radar is given in [5][7][3].

A bistatic geometry is shown in figure 2.1 for one transmitter, one receiver and one target. A segment of an ellipse indicating constant bistatic distance (range) is also shown. The baseline is a straight line (of length L) between the transmitter and the receiver. The distance (range) between the transmitter and the target is here denoted R_T, and the distance between the target and the receiver is R_R. The target's velocity vector ($\vec{v}$) is also shown. The bistatic angle β is the angle between the transmitter and the receiver seen from the target. The bistatic speed is measured in the direction of the bisector of the bistatic angle [5].

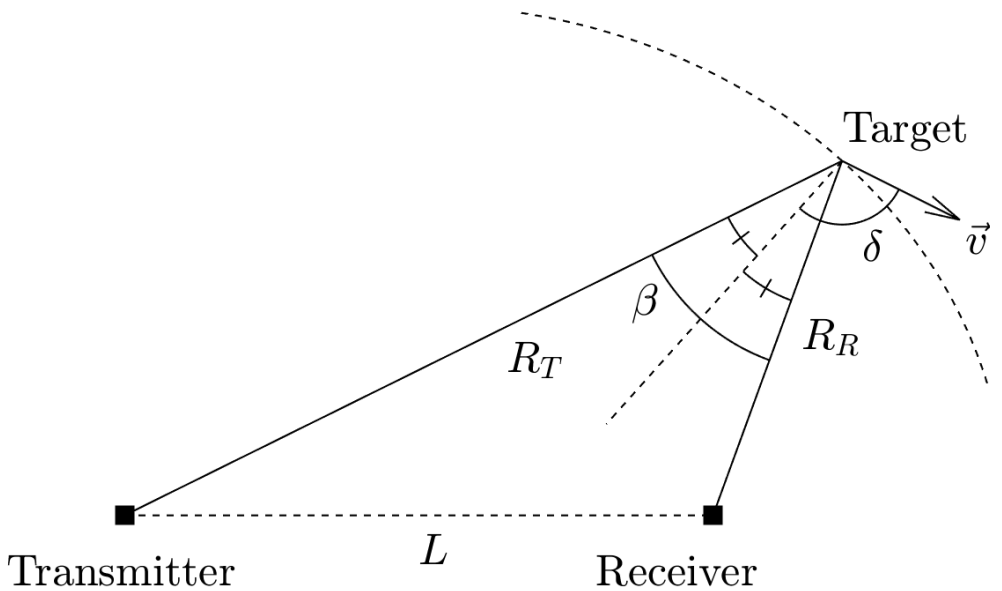

Figure 2.1: *Geometry for passive bistatic radar. The bisector of the bistatic angle β is shown with a straight, dashed line. The curved, dashed line indicates the rotational ellipsoid with constant bistatic range at the target.*

The definition used here for bistatic range is $(R_T + R_R - L)$, see figure 2.1. The range resolution in Cartesian coordinates for bistatic range in a direction with an angle ϕ (not shown in the figure) to the bisector is given by [5] (with misprint in [5] corrected)

$$\Delta R = \frac{c}{2B\cos(\beta/2)cos\phi} \tag{2.1}$$

where c is the speed of light and B is the bandwidth of the signal. The Cartesian velocity

resolution for the target along the bisector ($V_b = v\cos\delta$) for stationary transmitter and receiver is [5][7]

$$\Delta V_b = \frac{\lambda}{2T\cos(\beta/2)} \tag{2.2}$$

where λ is the wavelength of the signal and T is the integration time.

The detection of targets in passive bistatic radar is based on correlation of the signal from the transmitter (reference signal) and the return signal from the area of interest containing the echoes (surveillance signal). In many systems, the reference signal is measured with a directional antenna pointing towards the transmitter [7]. Some passive bistatic radar systems do not have separate antennas (or digitally formed beams) for the reference signal and the surveillance signal, but instead they are contained in the signal measured with the same antenna (element).

In either way, the direct signal (directly from the transmitter) is often present in the received surveillance signal through the surveillance antenna's main or side lobes and it is often strong compared to the echoes reflected from targets in the area of interest. In order to be able to detect weak targets, the receiver measuring the surveillance signal needs to be able to measure both very strong and very weak contributions in the received signals so its dynamic range needs to be high [7].

Assume that the bistatic range $r(t)$ as a function of time can be expanded in a Taylor series with its time derivatives of different orders at time $t = 0$ [7]:

$$r(t) = R + Vt + \frac{At^2}{2} + ... \tag{2.3}$$

where R is the bistatic range, V is the bistatic velocity and where A is the bistatic acceleration. The reflected radio frequency echo signal x_e^{RF} from a point object can then be written [7]:

$$x_e^{RF} = Re\left\{C_e^{RF} \cdot x_r\left(t - \frac{r(t)}{c}\right)\exp\left(i2\pi f_c\left(t - \frac{r(t)}{c}\right)\right)\right\} \tag{2.4}$$

where $x_r(t)$ is the transmitted signal in complex baseband representation (low centre frequency before up-converted to radio frequency, see below), C_e^{RF} is the relative amplitude of the echo from the object, and f_c is the upconversion frequency of the transmitted radio frequency signal.

In the reception process, the received real-valued signal is, in most systems, down-converted in one or several steps from the radio frequency band to a signal with lower centre frequency, where the centre frequency after the last down-conversion step often is of the same order of magnitude as the bandwidth of the signal or less (baseband signal). If the samples in the baseband signal are complex-valued (i.e. they are represented by complex numbers), then it is called complex baseband signal. The up- or down-conversion in frequency (corresponding to the factor $exp(i2\pi f_c t)$ in 2.4) is often done in hardware by mixing with a sinusoidal signal from a local oscillator possibly followed by filtering [8]. If complex baseband is used, then the sinusoidal signal from the local oscillator is shifted 90 degrees out of phase for the imaginary part of the complex baseband signal. A complex baseband signal can also be calculated in software from a real baseband signal.

After down-conversion and assuming that the bistatic range $r(t)$ can be approximated with the first two terms in its Taylor expansion (i.e. $r(t) \approx R + Vt$) during the integration time and that the baseband signal x_r in equation 2.4 is not influenced by the change in bistatic range during the integration time, then the complex baseband signal from the object can be written [7]

$$x_e(t) = C_e \cdot x_r\left(t - \frac{R}{c}\right) \cdot \exp\left(i2\pi\frac{V}{\lambda}t\right) \tag{2.5}$$

where C_e is a complex scale factor which is constant during the integration time. The reflected signal in baseband in this model is assumed to be equal to the transmitted baseband signal, $x_r(t)$, but scaled (first factor in equation 2.5), delayed (second factor) and Doppler-shifted (third factor).

The cross-ambiguity function is a cross-correlation between the received signal and the complex conjugate of the reference signal shifted by the distance (or corresponding delay) R in bistatic range and shifted by V in bistatic velocity (or frequency), see also section 2.2. The cross-ambiguity function in baseband between the received surveillance signal $x_s(t)$ and the reference signal $x_r(t)$ can be written [7]):

$$\psi(R,V) = \int_{-T/2}^{T/2} x_s(t) \cdot x_r^*\left(t - \frac{R}{c}\right) \cdot \exp\left(-i2\pi\frac{V}{\lambda}t\right)dt \tag{2.6}$$

where T is the integration time. The cross-ambiguity function is evaluated over some intervals in bistatic range and in bistatic velocity corresponding to the area of interest, creating a range-velocity diagram. A target in the area will give a strong correlation in equation 2.6 which then can be found by searching the range-velocity diagram for a correlation peak. The evaluation of the cross-ambiguity function corresponds to matched filtering and Doppler processing in active, pulsed radar [7].

2.1 Radar range equation

The radar range equation is fundamental for radars as it describes the relationship between the main system parameters and the ability to detect a target. It elaborates the Signal-to-Noise Ratio (SNR), which is the ratio between the power of the received signal P_r and the power of the noise P_n. The bistatic radar range equation can be written [3][5][7]

$$SNR = \frac{P_r}{P_n} = \frac{P_t G_t}{4\pi R_T^2}\frac{\sigma_b}{4\pi R_R^2}\frac{G_r\lambda^2}{4\pi}\frac{TB}{k_B T_s BL} \tag{2.7}$$

where parts of the last factor assume matched filtering, see below. The received signal power is proportional to the power of the transmitted signal P_t. It is assumed that the target is in the far field so that the power transmitted from the transmitter towards the target is approximately distributed with constant power over a solid angle in that direction. For a constant solid angle, the illuminated area will increase proportionally to the square of the distance from the transmitter. Hence, the power reaching the target

is inversely proportional to the square of the distance between the transmitter and the target R_T (and to factor 4π for the area of the sphere). The gain of the transmit antenna G_t is the ratio between the power density received at the target and the power density at that distance if the total transmitted power had been transmitted isotropically. The gain G_t also includes a reduction for power losses on the way between the antenna input and the output in the atmosphere. A part of the signal power reaching the target is reflected from the target into the direction of the receiver. This part is proportional to the bistatic radar cross section σ_b of the target (in that direction), which is expressed as an area and depends on the size, shape and materials of the target and on the polarisation of the signal and on how the target is rotated relative to the transmitter and the receiver. The signal power reflected from the target into the direction of the receiver is spread similarly to the transmitted signal explained above, so that the power reaching the receiver is inversely proportional to the square of the distance between the target and the receiver R_R (and factor 4π). The power received in the receiver antenna is proportional to the effective area of the antenna in the direction towards the target. The effective area is the physical antenna aperture area reduced by various losses. The relationship between the effective area A_e, the wavelength of the signal λ and the receiver antenna gain G_r can be written [8][9]

$$A_e = \frac{G_r \lambda^2}{4\pi}. \tag{2.8}$$

In all objects, charged particles exhibit random thermal motion and emit electromagnetic waves of different frequencies and polarisation [8][1]. These electromagnetic waves are called thermal noise. The noise is generated both externally in the surroundings of the radar and internally by randomly moving electrons in the radar system. At frequencies below the order of 1 GHz, man-made noise can dominate over the thermal noise while at higher frequencies, the thermal noise of the radar receiver is often the dominating received noise [7]. The thermal noise power spectral density (noise power per frequency) in the radar receiver is proportional to the system noise temperature T_s with Boltzmann's constant k_B as the proportionality constant. The power of the thermal noise P_n over the receiver effective bandwidth B can then be written $k_B T_s B$ [9].

The power of the received signal P_r in equation 2.7 is also decreased by various losses L which include losses from the atmosphere, the receiver and the signal processing [9].

An echo signal contribution from a target is integrated coherently in the cross-ambiguity function 2.6, while contributions from the noise are uncorrelated with the reference signal and are integrated incoherently. The number of samples, for which the different contributions are integrated coherently or incoherently, is proportional to the integration time T, thereby giving a proportional gain in the SNR. Increasing the signal bandwidth will also increase the power of the received signal proportionally if the signal's power spectral density is about the same, if a matched filter is used and assuming that the receiver effective bandwidth is increased accordingly so that it is kept slightly larger than the signal bandwidth. So the signal processing gain is proportional to the time-bandwidth product which then can be written as the product TB, which corresponds to the number of independent samples of the noise. In the next section, it is shown how the SNR can be calculated if the receiver effective bandwidth and the signal bandwidth are not about the same.

2.2 Matched filter

Receiver noise can often be accurately modelled with a normal (Gaussian) distributed random variable with zero mean added to each sample of the sampled signal, additive white Gaussian noise, with all frequency components having the same weight (white). Knowledge of the value of the white noise at one instant of time gives no knowledge of the value of the white noise at another instant of time. The linear shift-invariant (invariant to delays) operator that maximizes the SNR for a signal with white noise is the matched filter. The matched filter is the time-reversed complex conjugate of the transmitted signal. By cross-correlating the received signal with the matched filter, the delay, phase and amplitude of the signal reflected from a point target can be estimated.

Assume the noise is additive, zero mean white Gaussian noise $n(t)$ (in case of a complex-valued signal, the real and imaginary parts are independent and identically distributed). The response of a linear filter, with impulse response $h(t)$, to the signal reflected from a stationary point target can then be written

$$y(t) = \int \big(be^{i\phi}x(\tau - t_d) + n(\tau)\big)h(t-\tau)d\tau \tag{2.9}$$

where $x(t)$ is the transmitted and reflected signal, b is the amplitude of the received signal, ϕ is the phase relative to the transmitted signal and t_d is the time delay, see also [10][11]. Let R be the distance to the point target, then $t_d = 2R/c$ and $\phi = -4\pi R/\lambda$ where c is the speed of light and λ is the wavelength of the transmitted signal. Equation 2.9 can be transformed to the frequency domain, where the SNR can be calculated as [10]

$$SNR = \frac{b^2\left|\int X(\omega)H(\omega)d\omega\right|^2}{2\pi N_0 \int |H(\omega)|^2 d\omega} \tag{2.10}$$

where N_0 is the power spectral density of the noise.

Using the Cauchy-Schwarz inequality, the maximum SNR is attained when $H(\omega) = \alpha X^*(\omega)$, where α is an arbitrary constant. This is the matched filter in the frequency domain. Transforming back to the time domain gives

$$h(t) = \alpha x^*(-t) \tag{2.11}$$

which is the matched filter in the time domain.

If the receiver effective bandwidth B_r and the signal bandwidth B_s are not about the same, a simple indication of how the SNR can be estimated is given by noting that the integrand in the integral in the numerator in equation 2.10 is non-zero inside a frequency band of width less than or equal to the minimum of B_r and B_s. In that case, the numerator and the SNR scale quadratically with the minimum bandwidth of B_r and B_s, while the denominator scales with B_r.

2.3 Reference signal

As the results of evaluating the cross-ambiguity function (equation 2.6) depends on the reference signal, it is important that the reference signal has good quality, and is as clean as possible [5], with high SNR and without (possibly Doppler-shifted) multipath contributions. In many passive radar systems, the reference signal is measured with a directional antenna directed towards the transmitter. In some types of signals frequently used for passive radar, the transmitted signal is generated from a digital source and contains redundant information so that it is possible to correct and reconstruct the transmitted signal without the contribution from delayed echo signals and receiver noise. If the reference signal is demodulated (and maybe also decoded) with few uncorrected errors, a clean reference signal could be obtained by (coding and) modulating the signal again.

If the reference signal is not a radar signal, there might be features in the signal that could give rise to undesirable artefacts in the cross-ambiguity function, e.g. sidelobe peaks [5]. If the quality of the reference signal is sufficient, it might be possible to suppress these artefacts by manipulating the reference signal, thereby creating a mismatched filter.

Important characteristics to take into account when comparing different sources of illumination for passive radar include frequency, bandwidth, area coverage, signal strength, if the signal characteristics for passive radar purposes varies with time and the number of available transmitters visible in the same time. The characteristics for passive radar of broadcast and communication signals that use analogue modulation depend on the program contents transmitted at the moment.

3 Passive Synthetic Aperture Radar

The passive SAR image is produced using measurements of received echo returns and their corresponding (measured) positions together with a measured reference signal from a transmitting source and the positions of the source. The positions of the moving (and stationary) receiver or transmitter antennas need to be measured or known with high accuracy in order to calculate a SAR image. The accuracy needs to be better than of the order of a wavelength in order to avoid defocusing, if not compensated for in other ways.

For an airborne receiver, signals from additional transmitters may be received on altitude compared to on ground level. It may also be that some of these signals received on altitude uses the same frequency band, giving co-channel interference [5]. There may also be contributions from several different transmitters at different locations that transmit the same signal (but differently delayed at reception) if Single Frequency Network is used.

Often, there is a straight signal path from the transmitter to the receiver, making the direct signal (used for reference) very strong in the received signal. If a non-directional antenna is used for measuring the reference signal, then there will be contributions present from echoes with different signal paths giving rise to Doppler spreading, which can give inter-carrier interference if a multiple carrier signal is used. If the reference signal is received along with the surveillance signal in an airborne receiver, and the reference signal is demodulated and decoded with few uncorrected errors, then a clean reference signal

can be obtained without the need for a separate reference signal receiver platform, thus making the SAR system less complex. The strong direct signal is often significant in the surveillance signal, compared to the echoes, even if a directional antenna is used for the surveillance signal (discussed in section 5.2).

In a bistatic SAR image, some features may be different from what are seen than in monostatic SAR [5]. For example, there might be shadows from two directions from the same object in the bistatic SAR image, one in the direction from the transmitter and one in the direction from the receiver. The reflections from dihedral and trihedral corners between horizontal ground and vertical tree trunks or walls of buildings may also be less strong than in monostatic geometry [5], because of the non-zero bistatic angle (β in figure 3.1). This can be an advantage for example for finding targets in forests [12].

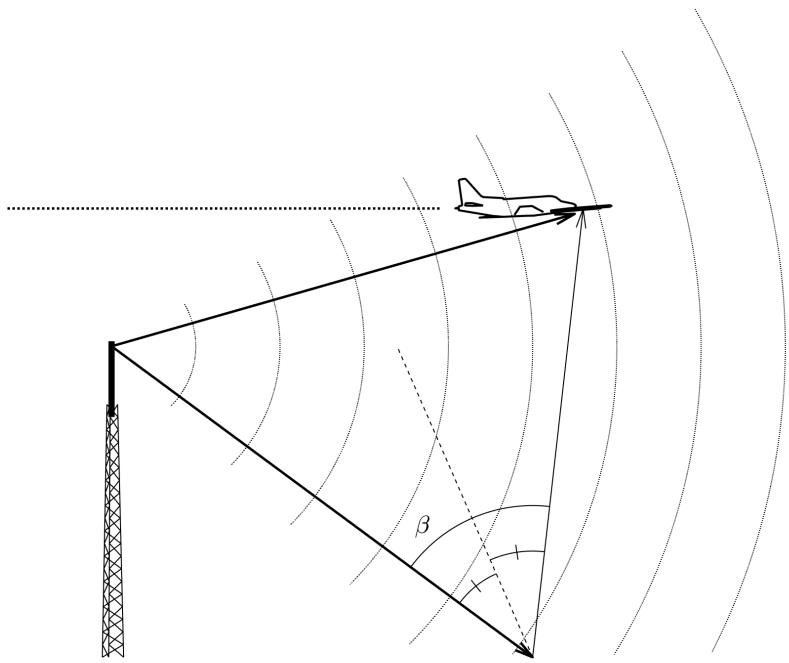

Figure 3.1: *Passive SAR geometry with stationary transmitter (on tower) and moving receiver (in aeroplane). An echo signal path and the direct signal path from transmitter to receiver are shown (arrows).*

For a stationary transmitter, the resolution in (one-way) range along the bisector of the bistatic angle is [4]

$$\Delta R = \frac{c}{2B\cos(\beta_m/2)} \tag{3.1}$$

where β_m is the bistatic angle of a target when the receiver is in the middle of the synthetic aperture, and where c is the speed of light and B is the signal bandwidth. The best

resolution is when $\beta_m = 0$.

The azimuth resolution in the direction of the velocity vector of the receiver relative to the target is [4]

$$\Delta A = \frac{\lambda}{2\omega_E T_d} \tag{3.2}$$

where ω_E is the effective angular speed of the receiver relative to the target, T_d is the radar dwell time on the target and λ is the wavelength of the centre frequency. The resolution in range and azimuth thereby depends on the target's position relative to the transmitter and the receiver positions.

4 Digital Video Broadcasting-Terrestrial

The digital TV standard Digital Video Broadcasting-Terrestrial (DVB-T) from European Telecommunications Standards Institute [6] uses Orthogonal Frequency Division Multiplexing (OFDM) modulation with 6817 parallel carriers in one symbol in the 8K transmission mode [6]. Out of the 6817 carriers, only 6048 are used for carrying data, which is pseudo randomly coded for each carrier. The rest, called pilot carriers and Transmission Parameter Signalling (TPS) carriers are there for helping decoding the signal (e.g. in multipath environments) and the pilots are sent with slightly higher average power. The frequency separation between two carriers in the 8K mode is $1/T_u$, where $T_u = 0.896$ ms is the duration of the useful part of the symbol. There is also a 2K mode with shorter symbol duration, giving a larger frequency separation between adjacent carriers. The DVB-T 8K mode signal is specified for a Doppler tolerance for high-speed reception, while the 2K mode has a Doppler tolerance making "extremely high" [6] speed reception possible. The DVB-T 8K mode is specified for being used with a single transmitter and in small, medium and large single frequency networks. Between each symbol (in time domain), a guard interval, which equals the cyclic continuation of a fraction ($\frac{1}{4}$, $\frac{1}{8}$, $\frac{1}{16}$ or $\frac{1}{32}$) of the useful part of the later symbol, is inserted. The required carrier-to-noise ratio (a measure of signal quality) to achieve a certain bit error rate for different choices of transmission parameters is given in [6]. The DVB-T standard specifies signals that allow 6 MHz, 7 MHz and 8 MHz spacing between TV channel centre frequencies. The nominal bandwidth of the 8K mode in the 8 MHz channel, which is mainly used in this thesis, is about 7.6 MHz.

The DVB-T standard has been further developed to the standard DVB-T2 [13], and there has been migration towards this standard in some countries [7]. The DVB-T2 standard is more complex and flexible than the DVB-T standard which means that demodulation (and modulation for reference signal in passive radar) is more difficult.

The number of transmitted DVB-T and DVB-T2 signal frequency bands in Sweden decreased from up to six in some transmitter locations to one or two when the largest pay television company Boxer stopped broadcasting in the terrestrial network in January 2025 [14] but instead moved to other distribution technologies. The number of available DVB-T and DVB-T2 signal frequencies with good ground level power in most areas in Sweden then decreased to one or two. Also, the commercial TV channel TV4 stopped

broadcasting in the terrestrial network in Sweden in January 2026 [15] but instead use other technologies for distribution.

4.1 DVB-T in passive radar

The OFDM modulation is relatively advantageous for passive radar applications as it resembles band-limited noise [7]. However, the DVB-T signal also contains pilot carriers and the cyclic continuation (guard interval), which give rise to artefacts in the cross-ambiguity function [16][17].

The transmitted signal can be reconstructed, for use as reference signal, by demodulating and decoding the received signal (using the in-built error correcting coding), then coding and modulating the signal again. However, some parts of the transmitted signal that might be desirable in a reference signal, for example from non-linearities in the transmitter, may also be removed in that process. In general, as long as the transmitter equipment transmits a signal that fulfils the requirements in the standard defining the signal, the signal can vary within the specified allowed limits of these requirements, see also [7]. For example, the drift between the local oscillator in the transmitter relative to the local oscillator in the receiver is taken into account in the remodulation for creating a reference signal [17].

Demodulating the DVB-T signal received makes it possible to improve the reference signal (section 2.3) for passive SAR by removing multipath echoes and noise but also to decrease artefacts that will be present in the SAR images when DVB-T signals are used in passive radar. These artefacts can be decreased by manipulating the reference signal so that it becomes a mismatched reference signal. Also, by using a transmitted signal with good quality, the (usually very strong) direct signal present in the surveillance signal can be suppressed, so that the effects of the direct signal in the images can be reduced.

In order to be able to demodulate and decode the received DVB-T signal with few uncorrected errors, a minimum ratio between the power of the signal and the power of the noise (carrier-to-noise ratio) is needed [6], depending on the parameters used by the transmitter for the transmission. In addition to noise, delayed multipath echoes may be present in the received signal depending on receiver antenna beam width. Also, if the receiver is moving these multipath echoes can give rise to Doppler spreading and spread power to adjacent carriers in inter-carrier interference, making the signal more difficult to demodulate depending on receiver antenna beam width, platform speed and centre frequency. If the receiver is flying on high altitude, other transmitters using the same frequency band might be present (e.g. in a single frequency network) and could interfere, making the signal additionally more difficult to demodulate.

The ambiguities in the cross-ambiguity function [16] from pilot carriers and guard intervals arise at certain positions in range (delay) and Doppler shift [17]. These ambiguities give rise to artefacts in the passive radar image. The artefacts from the pilots can be suppressed by using a mismatched reference signal where the power of the pilots has been reduced by a factor of $\frac{9}{16}$ [17] (as mentioned earlier, the pilots are transmitted with slightly higher average power than the data carriers).

The use of synthetic aperture will limit the effect of the artefacts from pilot carriers

as is discussed in [4] for the back-projection algorithm for SAR image formation. This is because of the range and phase variations of the artefacts are different from those of real targets so that the back-projection algorithm will severely defocus the artefacts [4][18]. An expression for how the quadratic phase error depends on the wavelength, the platform velocity, the range and the aperture time in a quasi-monostatic case is given in [18]. There it is found that the quadratic phase error in the cases shown is much higher than about $\pi/4$ required for defocusing, and that DVB-T signal demodulation, suppressing pilots and modulation again might not be necessary for synthetic aperture radar. Below, in section 5.5, an example of suppressing the pilot carriers in a SAR image from LORA is shown.

Several different techniques have been presented to improve construction of a reference signal from a DVB-T signal received with an airborne platform, for example using several antennas (as in section 5.4 below) or using expansion in basis functions [19].

5 Passive SAR with the LORA system

The radar system LORA (LOw frequency RAdar) is an experimental radar system designed and built by the Swedish Defence Research Agency (FOI). It is installed in an aeroplane and uses two unique, specially designed antenna booms which are mounted outside the front of the aeroplane.

The LORA system could be operated in two different configurations, with two different pairs of booms requiring partly different hardware [20][21]. One pair of booms was reused from the older SAR system CARABAS II and is for frequencies in the range 20-90 MHz where each boom carries a biconical antenna. Inside each antenna boom in the other pair (configuration for VHF and UHF bands) are five wide-beam antenna elements, out of which three antenna elements are used for receiving radar echoes, and the other two are used for transmitting signals (in active mode). The antenna elements in one of the booms are for frequencies in the range 200-400 MHz while the antenna elements in the other boom are for frequencies 400-800 MHz. Reflectors along one side of the fixed, biconical antenna elements in both booms direct them down towards the left of the aircraft. The LORA system uses frequencies within one 80 MHz band at a time, but can change 80 MHz band from pulse to pulse. The possible LORA 80 MHz bands have centre frequencies (f_{cLORA}) of 270, 320, 400, 480, 560, 640, 720 and 800 MHz. The receiver in the LORA system has eight separate channels. At reception, the signals from the antenna elements are selected with switches and down-converted with selected centre frequencies to signals with bandwidth of 10 MHz and then sampled and registered in 12-bit real-valued samples at a rate of 25.6 MHz. The possible centre frequencies of the 10 MHz bands can be written $f_{cLORA} - 1.28 \text{ MHz} + m_{LORA} \cdot 5.12 \text{ MHz}$, where m_{LORA} is an integer so that the frequency is within the 80 MHz band. The LORA system can simultaneously sample and register up to eight different signals each with individual centre frequencies selected within the same 80 MHz band. The registration is designed for active radar mode where the echo signal from each pulse is saved in a data packet of up to 4096 samples, and along with each pulse some information about the pulse (time, used frequency etc.) is registered together with the data. For the demodulation of DVB-T signals, it is needed to take into account that the received signal is undersampled so that the high frequencies become low

frequencies in the sampled signal and vice versa and that there is a non-integer number of samples with LORA's sample rate during the useful part of one DVB-T symbol (T_u).

A Global Positioning System (GPS) receiver and an inertial measurement unit are also integrated in the LORA system and used for making measurements along the flight path so that the positions and orientations of LORA's antenna elements can be calculated with high accuracy.

The LORA system uses stripmap collection, so the aeroplane is typically flown along a straight (flight) path with its fixed antenna beam(s) pointing broadside. Further descriptions of the LORA system can be found in [22], [20] and [21].

Several measurement campaigns with LORA with the 20-90 MHz antenna boom pair or the VHF and UHF antenna pair have been performed over the years. Campaigns for experiments with LORA in configuration for mono-static, active SAR [22], for experiments with LORA in bistatic SAR arrangement together with other airborne systems [23], experiments with LORA in passive SAR configuration [24][25][26][20], comparison between active and passive SAR [27][21], combined with airborne moving target detection [28], and campaigns with several arrangements [24][29]. Experiments with LORA in both active and passive SAR modes have been made during the same flight [21], and also intermittently (every few seconds) during the same run.

5.1 The LORA airborne SAR system in passive mode

Since the first experiments with LORA in passive mode in year 2012 [24], measurement campaigns in several different locations have been carried out by FOI where the illuminators have been TV broadcasting transmitters that transmit DVB-T or DVB-T2 signals.

In LORA, it is not always possible to select the receiver centre frequency so that it coincides with the DVB-T signal centre frequency. In Sweden, the DVB-T and DVB-T2 centre frequencies can be written $(474 + m_{DVB} \cdot 8)$ MHz (see also [6]), where m_{DVB} is an integer, which means that not all broadcast DVB-T or DVB-T2 bands are close to the possible LORA centre frequencies. For the measurement campaigns, if possible, the recorded digital-TV signals were chosen so that there were at least two different TV signals, transmitted from the same location with sufficient power in area of interest, preferably transmitted using the DVB-T standard and not the DVB-T2 standard, completely within LORA's feasible 10 MHz bands within the same of LORAs 80 MHz bands (so that they could be recorded simultaneously).

During some of the field experiments with LORA, the direct DVB-T signal was recorded with a separate, stationary receiver on the ground connected to a directional antenna. The direct signal could then be recorded with high carrier-to-noise ratio so that it was easy to demodulate with few uncorrected errors and not necessary to decode.

As a reference signal for making passive SAR images, either the recorded signal from the flying platform was used to correlate with (in autocorrelation) or, in the case of a ground receiver, the signal recorded from the ground receiver was used to correlate with. Demodulating the DVB-T signal recorded by LORA makes the SAR system less complex as there is no need for a ground receiver.

As mentioned above for LORA in active mode, along with each pulse some information

about the pulse (time, used frequency etc.) is registered together with the data. Also in passive mode, because of the hardware, this pulse information needs to be registered along with the data, thus replacing 40 measured samples. This means that the LORA system cannot save samples completely continuously but, at the best, for every 4096 samples, 4056 samples are registered and 40 consecutive samples (about 1 %) are thrown away and are missing. During the useful part of one DVB-T symbol (T_u), between 200 and 240 samples are missing. The portion of missing samples is about 1 %, but although the positions of the missing samples are known, it is challenging to demodulate the signal even if the signal is recorded from a stationary platform. If the missing samples are represented by values different from the received but not recorded (missing) samples, the carriers will spread in frequency so that the separation in frequency between the carriers might be decreased and the carriers will interfere with each other (also power from strong signals in adjacent frequency bands (possibly other DVB-T signals) could interfere to small extent in frequency domain through convolution). Demodulating a DVB-T-signal with the missing samples set to zero was investigated in paper A. An algorithm for reconstructing the missing samples was proposed in paper B, see section 5.3.

If the missing samples are replaced by zeroes in the LORA signal and it is auto-correlated without being demodulated, then the 1 % missing samples will decrease the result of the auto-correlation with between about 1 and 2 %, depending on whether the missing samples overlap or not.

There are additional challenges to demodulate a DVB-T signal recorded on a flying platform. The signals are received in LORA's wide-beam antenna elements and contain frequency shifted multipath (Doppler) contributions from echoes that, although they are weaker, could make the carriers spread in frequency. The DVB-T signals that have been recorded with the LORA system use the DVB-T 8K mode signal which is specified for a Doppler tolerance for high-speed reception [6]. The maximum Doppler frequency shift can be approximated with $f_c \cdot v/c$, where f_c is the DVB-T signal centre frequency, v is the receiver speed and c is the speed of light. When recording DVB-T signals, the LORA platform has been flown with ground speeds mostly between 120 m/s and 160 m/s.

For the example in section 5.4, the ground speed is about 160 m/s and the DVB-T centre frequency is 594 MHz (received with LORA 10 MHz band with centre frequency 594.56 MHz), giving a maximum Doppler shift spread of about ± 317 Hz. The maximum total Doppler spread is $2f_c \cdot v/c \approx 634$ Hz which is about 57 % of the frequency separation between two carriers in the 8K mode $1/T_u = 1/0.896 \cdot 10^{-3} \approx 1120$ Hz as mentioned in chapter 4. The Doppler spread makes the carriers lose their orthogonality and interfere with each other. The strengths of the signal contributions within this Doppler spread depends on the distance to the echoing objects, their bistatic radar cross section, the receiver antenna gain pattern (factors in equation 2.7) and the direction of the antenna which also depends on the velocity of the wind where the aeroplane is flown.

In addition, when recording DVB-T signals, the LORA platform has been flown at altitudes mostly between 2800 m and 3800 m above ground where signals from transmitters further away within the same DVB-T frequency band might also be received and interfere, for example if single frequency network is used. On the ground, these signals from transmitters further away normally have lower signal strength. During a guard interval (cyclic prefix), the signal travels a distance of cT_u/N_g where N_g is the denominator for

the guard interval duration. If two identical signals are transmitted at the same time, but one of them travels more than cT_u/N_g longer distance to the receiver than the other, then when the start of the useful part of a symbol in the first signal is received, the second signal will still carry the previous symbol, giving rise to inter-symbol interference. For example, with the shortest guard interval of 1/32, this distance is only $cT_u/32 = 8.4$ km. Strong signal contributions from multipath echoes or single frequency network signals with delays longer than the guard interval make demodulation more difficult.

In the case of no ground receiver, it can be expected that the demodulated, corrected and modulated reference signal will be better than if the signal itself is used as reference signal since noise and multipath echoes with different Doppler shifts from a large area will be removed.

5.2 Effects of improving the reference signal quality

As written above, for the LORA SAR system with no directional antenna, both the surveillance signal and the reference signal are received with the same wide-beam antenna(s). For SAR image formation, either the surveillance signal(s) received in the wide-beam antenna(s) is used in autocorrelation or the signal recorded in a separate ground receiver with directional antenna is used as reference signal in cross-correlation with the surveillance signal(s). With a sufficiently good or improved reference signal that resembles the transmitted signal, the correlations can be improved, thereby improving image quality and target detections. If the reference signal can be demodulated with few uncorrected errors, then noise, Doppler spread multipath clutter and interfering signals received on the altitude of the aeroplane can be removed from the reference signal. The artefacts from the pilots can also be suppressed by reducing the power of the pilots in the reference signal (sections 4.1 and 5.5).

Improving the reference signal can also improve the suppression of the often very strong contribution from the direct signal in the surveillance signal. The contribution from the direct signal in the surveillance signal is often so strong that it is visible in the passive SAR image, thus suppressing the direct signal in the surveillance signal can improve the image [4]. An objective could be to suppress the strength of the direct signal to about the same level as the receiver noise [5]. Suppressing the interference from the direct signal in the surveillance signal can be done by subtracting the reference signal (multiplied with a constant) from the surveillance signal [7]. However, if the reference signal differ from transmitted signal then some target echo information could get lost too. There are several different algorithms for this [7][4], and some of them benefit from an improved reference signal. Several other means for suppressing the interference from the direct signal exist including steering the beam with an antenna array, using physical shielding of the antenna and using different polarisations [5].

5.3 Reconstruction of missing samples

As discussed above (section 5.1), it is desirable to demodulate the recorded signal with few uncorrected errors in order to be able to create a clean radar reference signal that

can suppress the artefacts from the signal structure. As samples are missing in the data sampled by LORA, it makes it more difficult to demodulate the DVB-T signals. It was shown with simulations in paper A (summary in section 6.1) that with about the same amount of missing samples as in the LORA system and above, the bit error rate of the decoded DVB-T symbols increases rapidly with the amount of missing samples even if no noise is present. Reconstruction of the transmitted signal before missing the samples is therefore desirable.

For a linear time-invariant communication channel, complex exponentials at different frequencies separated by an integer multiple of the reciprocal of the interval length are orthogonal [30], which is utilised in OFDM. Taking into account, as a part of the communication channel, that samples are missing makes the communication channel time-variant but preserves linearity. A lot of research about reconstruction of missing samples was found (for example [31]), but not for OFDM signals.

In paper B, an algorithm for reconstruction of missing samples in OFDM signals is proposed, and a summary is found in section 6.2. The proposed algorithm makes use of the OFDM signal structure with many parallel carriers, treats the real and imaginary parts of the complex amplitudes of the data carriers separately, and optimises the missing samples so that the data carriers' real and imaginary parts with highest absolute values come close to a square circumscribing the constellation. The algorithm was developed using basic ideas from continuous optimization, numerical analysis, signal processing and probability theory together with very simple observations from looking at diagrams over spread carriers in QAM-constellations. Some of the work and ideas behind the algorithm proposed in paper B is described below. As there are several different factors that make demodulation of the LORA signal difficult (section 5.1), it was assumed that the error correcting codes would be needed to take care of other distortions of the signal so that trying to recover or estimate the missing samples could be worthwhile doing. Since the data in the symbols change randomly from DVB-T symbol to symbol, and the data carriers make up a lot of the contents in a symbol, it was assumed that a successful solution would need to operate on one symbol at a time and that using statistics over several symbols would be less useful. Among standard methods for estimating missing samples in band-limited signal is the method of least squares ([31]). It was found that the band-limitation property of the measured signal (before missing samples) was not sufficient for solving the problem with the method of least squares as the condition number increase extremely rapidly with the number of missing samples. However, it was quickly found that there was enough information left (after missing samples) in the signal for solving the problem. That was found by creating an optimisation problem with an object function and the missing samples as unknowns. The created object function depended simply on the maximum absolute value of the real and imaginary parts of all data carriers in the constellation diagram. The algorithm used for solving this optimisation problem converged to a solution but very, very slowly. In order to try to decrease the convergence time at least a factor of one thousand times, the method of least squares was tried again but this time exploring an idea of adding extra equations in the object function where quite certain, but not completely certain, real or imaginary parts of the complex amplitudes of the measured data carriers were treated as certain, in order to improve the condition number but still leave the pilot and TPS carriers for their intended uses (like

channel compensation). In this way, information about the outermost, peripheral points in the constellation of data carriers together with the band-limitation property is used in a continuous optimisation. The complex amplitudes are separated in real and imaginary parts which are treated individually and differently depending on their absolute values. This is the algorithm proposed in paper B, summarised in section 6.2.

5.4 Demodulation of signals recorded in aircraft

The proposed algorithm for reconstruction of missing samples was applied to a real DVB-T signal transmitted in the 8K mode and received with the flying LORA system. Signals from three antenna elements with missing samples were combined and demodulated (the subcarrier symbols were extracted but not decoded). Before the proposed algorithm was applied, the start of each DVB-T symbol needed to be found (time synchronisation) together with the frequency shift needed to put the OFDM subcarriers on integer frequencies in the frequency domain (frequency synchronisation), also taking into account that LORA has a non-integer number of samples per DVB-T symbol. After synchronisation in time and frequency, the signal was transformed to the frequency domain and equalised.

In figure 5.1 below, preliminary results from demodulating and recovering samples from a DVB-T symbol received with the flying LORA system are shown. The signal is recorded when LORA is flown with a ground speed of about 160 m/s and the DVB-T centre frequency is 594 MHz. The signals from three receiver antennas have been combined in a simple, non-optimal way, and the algorithm for recovering missing samples was used in only one iteration. The results have later been improved by improving the method for combining the receiver signals and running more iterations. A DVB-T symbol measured by LORA misses between 200 and 240 real-valued samples. The particular symbol shown in figure 5.1 misses 240 samples which are more difficult to accurately estimate than 200 missing samples.

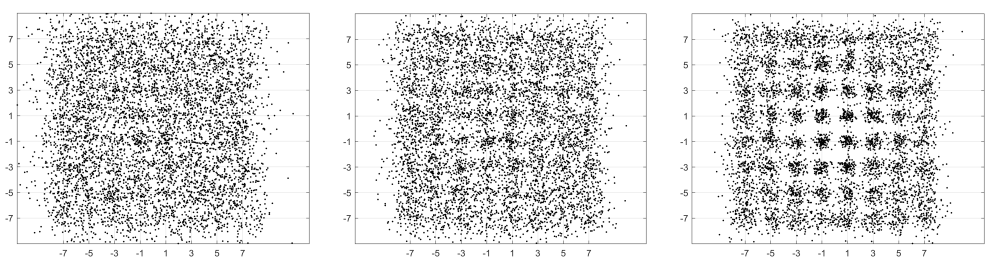

(a) *With signal from one receiver*

(b) *With signals from three receivers combined*

(c) *With three receivers and recovered samples*

Figure 5.1: *Constellation diagram from one DVB-T symbol received by the flying LORA system. The demodulation is based on (a) the signal from one receiver, (b) signal from three receivers combined in a simple, non-optimal way, (c) the same combined signal after first iteration with the algorithm for recovering missing samples proposed in paper B.*

5.5 Using demodulated signal as reference signal

The signal demodulated in the previous section was improved by rounding the complex amplitudes in the constellation diagrams to their nearest ideal constellation point. This rounded signal was then also manipulated by decreasing the power of the pilot carriers. Then the demodulated, rounded and possibly manipulated signal was modulated to baseband again for use as a reference signal. Before being used as a reference signal, the DVB-T symbols were synchronised in time and shifted back in frequency, again taking into account that LORA has a non-integer number of samples per DVB-T symbol (previous section).

Figure 5.2 shows how a passive SAR image using the same LORA signal is improved in two steps. The images show the absolute value of the (complex valued) results of the correlations for an area of 4.1x4.1 km. The SAR image integration time is 2.8 s.

In figure 5.2a, the signal received in the flying LORA system has been autocorrelated, i.e. correlated with itself. The received signal contains noise, clutter from multipath echoes with different Doppler shifts from a large area and also artefacts from the structure of the DVB-T signal itself.

In figure 5.2b, the signal received in the flying LORA system has been cross-correlated with the demodulated, rounded and modulated reference signal. The reference signal was created by equalising and demodulating the signal using the pilot carriers so that the underlying constellation becomes visible, then rounding the complex amplitude of each carrier in the DVB-T frequency band to the nearest ideal constellation point and then finally modulating the signal again with the same delay and frequency shift (including Doppler shift) as in the received signal.

Figure 5.2c shows the result of cross-correlation between the received signal and the reference signal where the demodulated and rounded complex amplitudes of the pilot carriers have been multiplied by $\frac{9}{16}$ before modulating the signal again. The power of the pilots is thereby reduced to the same average power as for the data carriers in the transmitted constellation. It is visible that the strong artefacts that together resemble a sector of circle segments in figures 5.2a and 5.2b have been reduced by reducing the power of the pilot carriers.

The image in figure 5.2d shows the absolute value of the difference between the absolute values of each point with (figure 5.2b) and without (figure 5.2c) pilot suppression. The absolute difference has then been decimated from 2048×2048 points to 128×128 points by taking the maximum value of 16×16 points in order not to miss individual strong elements in the image. Each picture element then covers an area of 32×32 m.

The colour scales in these images in figure 5.2 have been given upper limits that are lower than the strongest pixels. It is visible that the change shown in figure 5.2d could be of about the same order of magnitude as the values shown in figure 5.2b and that suppressing the pilots gives a noticeable effect in this example. It has not been further analysed which ambiguities from the DVB-T signal that give rise to the artefacts in figures 5.2a and 5.2b that are changed by suppressing the pilots.

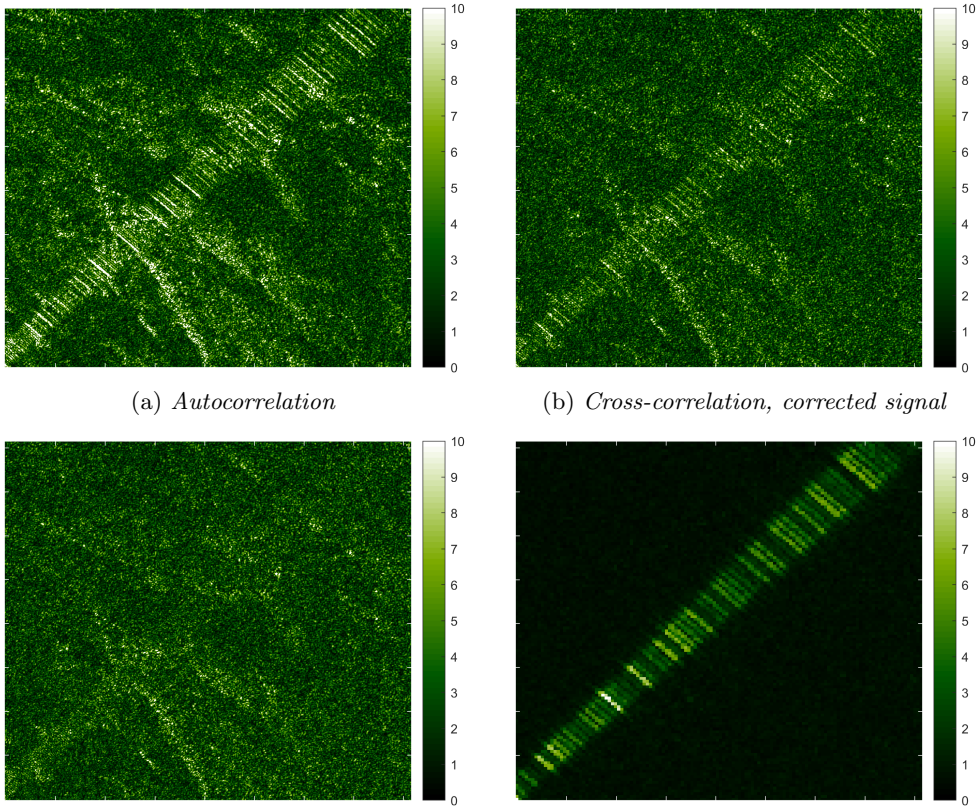

(a) *Autocorrelation*

(b) *Cross-correlation, corrected signal*

(c) *Cross-correlation, suppressed pilots*

(d) *Absolute change due to pilot suppression*

Figure 5.2: *Passive SAR images from LORA showing the absolute values of the results from (a) auto-correlation (b) cross-correlation with demodulated, corrected and modulated signal (c) cross-correlation with corrected signal in which the power of the pilot carriers has been reduced (d) absolute difference between the absolute values of each point from cross-correlations with and without pilot suppression.*

6 Summary of Appended Papers

6.1 Paper A

In paper A, it is shown with simulations that missing samples (or rather, corresponding samples set to zero) in DVB-T symbols increase the deviations in the constellation diagram, thus making demodulation more difficult. It is shown with simulations that with about the same amount of missing samples as in the LORA system (i.e. about 1 %) and above, the bit error rate of the decoded DVB-T symbols increases rapidly with the amount of missing samples even if no noise (except quantisation errors) is present. Diagrams over

how the bit error rate increases with the amount of added white Gaussian noise for no missing samples and for 28 missing samples per 4096 samples are shown.

In the simulations, an existing implementation of DVB-T signals in the GNU Radio tools was used in which a simulated DVB-T signal was generated. The generated signal was then resampled to the LORA sampling rate where a variable amount of white Gaussian noise was added and a variable number of consecutive samples were set to zero every 4096 samples (to resemble the LORA system in passive mode). The signal was then resampled back to the sampling rate used by the DVB-T implementation in the GNU Radio tools, where it was demodulated and decoded using hard decision. The resulting decoded signal was then compared with the generated signal, and the results are described in paper A.

6.2 Paper B

In this paper, an algorithm is proposed for reconstruction of an OFDM signal (in particular a DVB-T signal) in which various portions of samples are missing. The proposed algorithm optimises the unknown missing samples with the method of least squares, using an objective function in the frequency domain. The objective function works on the useful part of one DVB-T symbol at a time and consists of the weighted sum of two parts. The first part is the energy in frequencies outside the DVB-T band and outside any other strong signal in the sampled data. The second and novel part uses data carriers spread to the outermost, peripheral regions of the constellation of data carriers. In the algorithm, a circumscribing square is defined to be the smallest square that circumscribes the ideal QAM constellation grid (pilot and TPS carriers excluded). A second square is defined to be concentric to the circumscribing square and of chosen size (which is a real, scalar parameter of the algorithm). The second part of the objective function is the sum of the square of the shortest distances (along the real or imaginary axes) to the circumscribing square for all data carriers spread outside the concentric square. The circumscribing square thus stands for the desired values of the real or imaginary parts of data carriers outside the concentric square. In this way, there is a non-zero probability that a desired value for the real or imaginary part of a data carrier outside the concentric square is not correct, that is, the associated extra equation is incorrect. Mathematical expressions for the ratio of the incorrect to correct extra equations are derived for a channel with white Gaussian noise, and it is shown that this ratio is constant along the side of the concentric square. See also section 5.3 above for more information about the algorithm.

The second part of the objective function is shown with simulations to improve the accuracy of the algorithm by improving the condition number, which is shown to be improved more than a factor ten thousand millions compared to using the least square method with the first part only.

The algorithm is evaluated both with simulated signals and with a real signal measured with LORA connected to a stationary directional antenna. The algorithm is shown to significantly improve the DVB-T signal with only a few (one or two) iterations. The result of the algorithm is also further decoded using several other algorithms (for example the Viterbi decoding algorithm for the convolutional codes) showing that the proposed algorithm gives significant improvement.

Graphs are shown how the condition number (with respect to matrix inversion of the system of linear equations in the method of least squares) is improved several orders of magnitude when the number of extra equations in the second part of the objective function is increased. Graphs are shown how the number of extra equations is related to the chosen size of the concentric square for different values of SNR in simulations with white Gaussian noise added.

Graphs are also shown how the Root Mean Square (RMS) errors and the ratios of data carriers closer to another constellation grid point than the correct one, decrease after one and after two iterations with the proposed algorithm. The results also show that the algorithm is not very sensitive to a small portion of incorrect extra equations among the correct ones.

Results are shown from simulations of a passive radar where the same received signal, with target echoes and samples missing, is used as input for both reference and surveillance signal. Signals reconstructed with the proposed algorithm, with and without reduced pilot carriers, are used as reference signal in cross-correlations with the received signal. The result from using reconstructed signal and a signal with no samples missing, no noise and no targets are very similar. A strong ambiguity peak in the cross-ambiguity function of the (8K mode) DVB-T signal was shown to be suppressed when pilot carriers were reduced.

Results are also shown from when the algorithm is applied to a real measured signal received by the LORA system connected to a stationary, directional antenna where e.g. multipath effects are present, requiring time and frequency synchronisation and equalisation using pilot carriers. The estimated RMS error is shown to decrease in two iterations.

After simulations with further decoding, graphs show the minimum SNR, the maximum portion of consecutive missing samples and the number of iterations (1, 2, 3 and 6 iterations) required for achieving less than one uncorrected error event per hour after even further decoding.

7 Conclusions and Future Work

Construction of a reference signal for passive Synthetic Aperture Radar based on demodulating DVB-T signals missing a portion of the recorded samples has been investigated and reported in this thesis. A novel algorithm for demodulating a DVB-T signal with samples missing has been discussed and has been shown to work for constructing a good reference signal. The reference signal was constructed by demodulating a DVB-T signal received on the flying LORA platform and examples of constellation diagrams of the demodulated signal were shown. The demodulated signal was then improved by rounding each carrier to the nearest ideal constellation point and decreasing the power of the pilot carriers. Then it was modulated again to make a reference signal that was shown to suppress artefacts from the signal structure in a SAR image example.

A number of factors that influence the ability to demodulate DVB-T signals recorded with a flying platform have been discussed. Other improvements that can be made in the passive SAR images by making a reference signal from demodulating the received DVB-T

signal have also been discussed.

Future work may include improving the demodulation of the signal shown in section 5.4, possibly by decoding the signal using the in-built error correcting codes. Algorithms using the demodulated signal for suppressing artefacts in the passive SAR image from interference from the strong direct signal may also be implemented.

References

[1] J. A. Scheer and W. A. Holm, "Introduction and radar overview," *Principles of Modern Radar: Basic Principles*, M. A. Richards, J. A. Scheer, and W. A. Holm, Eds. The Institution of Engineering and Technology, 2010, pp. 3–58.

[2] W. L. Melvin and J. A. Scheer, "Radar applications," *Principles of Modern Radar: Vol. III: Radar Applications*, W. L. Melvin and J. A. Scheer, Eds. The Institution of Engineering and Technology, 2014, pp. 1–16.

[3] H. Griffiths and C. Baker, "Passive bistatic radar," *Principles of Modern Radar: Vol. III: Radar Applications*, W. L. Melvin and J. A. Scheer, Eds. The Institution of Engineering and Technology, 2014, pp. 499–541.

[4] M. Antoniou and G. Atkinson, "Passive synthetic aperture radar with DVB-T transmissions," *Passive Radars on Moving Platforms,* D. Cristallini and D. W. O'Hagan, Eds. The Institution of Engineering and Technology, 2023, pp. 141–174.

[5] H. D. Griffiths and C. J. Baker, *An introduction to passive radar*, 2nd ed. Artech House, 2022.

[6] *Digital Video Broadcasting (DVB); Framing structure, channel coding and modulation for digital terrestrial television,* ETSI EN 300 744 V1.6.2 (2015-10)*,* European Telecommunications Standards Institute, ETSI, 2015.

[7] M. Malanowski, *Signal Processing for Passive Bistatic Radar,* Artech House, 2019.

[8] R. J. Sullivan, *Radar Foundations for Imaging and Advanced Concepts*. The Institution of Engineering and Technology, 2004.

[9] J. A. Scheer, "The radar range equation," *Principles of Modern Radar: Basic Principles*, M. A. Richards, J. A. Scheer, and W. A. Holm, Eds. The Institution of Engineering and Technology, 2010, pp. 59–86.

[10] B. M. Keel, "Fundamentals of pulse compression waveforms," *Principles of Modern Radar: Basic Principles*, M. A. Richards, J. A. Scheer, and W. A. Holm, Eds. The Institution of Engineering and Technology, 2010, pp. 773–834.

[11] J. G. Proakis, *Digital Communications*, 3rd ed. McGraw-Hill, 1995.

[12] L. M. H. Ulander et al., "Signal-to-clutter ratio enhancement in bistatic very high frequency (VHF)-band SAR images of truck vehicles in forested and urban terrain," *IET Radar, Sonar & Navigation,* vol. 4, no. 3, pp. 438–448, 2010.

[13] *Digital Video Broadcasting (DVB); Frame structure channel coding and modulation for a second generation digital terrestrial television broadcasting system (DVB-T2),* ETSI EN 302 755 V1.4.1 (2015-07)*,* European Telecommunications Standards Institute, ETSI, 2015.

[14] Regeringen, *Kommittédirektiv Tilläggsdirektiv till Distributionsutredningen 2024 (Ku 2024:02), Beslut vid regeringssammanträde den 3 juli 2025*, Dir. 2025:69, Swedish, 2025.

[15] Mediemyndigheten, *Marksänd tv, Information om tillstånd att sända tv för tillståndsperioden 1 januari 2026–31 december 2033*, Swedish, 2025.

[16] C. Bongioanni, F. Colone, D. Langellotti, P. Lombardo, and T. Bucciarelli, "A new approach for DVB-T Cross-Ambiguity Function evaluation," *Conference Proceedings - 6th European Radar Conference, EuRAD 2009, (2009)*, pp. 37–40.

[17] J. E. Palmer, H. A. Harms, S. J. Searle, and L. M. Davis, "DVB-T passive radar signal processing," *IEEE transactions on signal processing,* vol. 61, no. 8, pp. 2116–2126, 2013.

[18] Y. Fang, G. Atkinson, A. Sayin, J. Chen, P. Wang, M. Antoniou, and M. Cherniakov, "Improved passive SAR imaging with DVB-T transmissions," *IEEE transactions on geoscience and remote sensing,* vol. 58, no. 7, pp. 5066–5076, 2020.

[19] C. Berthillot, A. Santori, O. Rabaste, D. Poullin, and M. Lesturgie, "BEM reference signal estimation for an airborne passive radar antenna array," *IEEE transactions on aerospace and electronic systems,* vol. 53, no. 6, pp. 2833–2845, 2017.

[20] L. M. H. Ulander, P. Frölind, A. Gustavsson, A. Haglund, and R. Ragnarsson, "Passive synthetic-aperture radar for detection of ground vehicles," *International Conference on Radar Systems (Radar 2017)*, pp. 1–4.

[21] L. M. H. Ulander, P.-O. Frölind, A. Gustavsson, A. Haglund, R. Ragnarsson, and T. Sjögren, "Ground mapping using active and passive UHF-band SAR," *2020 IEEE International Radar Conference (RADAR)*, pp. 524–529.

[22] L. M. Ulander et al., "The VHF/UHF-band LORA SAR and GMTI system," *Algorithms for Synthetic Aperture Radar Imagery,* vol. 5095, no. 1, SPIE, 2003, pp. 206–215.

[23] R. Baqué, P. Dreuillet, O. R. du Plessis, H. Cantalloube, L. Ulander, G. Stenström, T. Jonsson, and A. Gustavsson, "LORAMbis A bistatic VHF/UHF SAR experiment for FOPEN," *2010 IEEE Radar Conference*, pp. 832–837.

[24] L. M. H. Ulander, P.-O. Frölind, A. Gustavsson, R. Ragnarsson, and G. Stenström, "VHF/UHF bistatic and passive SAR ground imaging," *2015 IEEE Radar Conference (RadarCon)*, pp. 0669–0673.

[25] L. M. H. Ulander, P.-O. Frölind, A. Gustavsson, R. Ragnarsson, and G. Stenström, "Airborne passive SAR imaging based on DVB-T signals," *2017 IEEE International Geoscience and Remote Sensing Symposium (IGARSS)*, pp. 2408–2411.

[26] P.-O. Frölind, A. Gustavsson, A. Haglund, R. Ragnarsson, and L. M. H. Ulander, "Analysis of a ground target deployment in an airborne passive SAR experiment," *2017 IEEE Radar Conference (RadarConf)*, pp. 0273–0278.

[27] L. M. H. Ulander, P.-O. Frölind, A. Gustavsson, A. Haglund, and R. Ragnarsson, "Active and passive UHF-band SAR for ground surveillance," *EUSAR 2018; 12th European Conference on Synthetic Aperture Radar*, pp. 1481–1484.

[28] T. K. Sjögren, P. O. Frölind, R. Ragnarsson, A. Haglund, A. Gustavsson, L. M. H. Ulander, V. T. Vu, and M. I. Pettersson, "Simultaneous passive SAR imaging and detection of airborne targets," *International Conference on Radar Systems (Radar 2017)*, pp. 1–5.

[29] L. M. H. Ulander, M. J. Soja, A. Gustavsson, E. Blomberg, and J. E. S. Fransson, "Mono- and bistatic UHF-band SAR measurements of a hemi-boreal forest," *2015 IEEE International Geoscience and Remote Sensing Symposium (IGARSS)*, pp. 5079–5082.

[30] U. Madhow, *Fundamentals of digital communication*. Cambridge University Press, 2008.

[31] P. J. S. G. Ferreira, "Iterative and noniterative recovery of missing samples for 1-D band-limited signals," *Nonuniform Sampling*, F. Marvasti, Ed. Springer US, 2001, pp. 235–281.